Electromagnetically induced transparency in a three-level lambda system with permanent dipole moments

Fengxue Zhou, Yueping Niu,[a] and Shangqing Gong[b]
State Key Laboratory of High Field Laser Physics, Shanghai Institute of Optics and Fine Mechanics, Chinese Academy of Sciences, Shanghai 201800, China

(Received 3 March 2009; accepted 20 June 2009; published online 16 July 2009)

Electromagnetically induced transparency in a three-level Λ-type molecular system with nonzero permanent dipole moments is investigated. It is shown that in the (2+2)-transition processes, when the sign of d_{21}, the difference in permanent dipole moments of the probe transition, is positive, perfect electromagnetically induced transparency with steep normal dispersion could be obtained under specific conditions. In contrast, when the sign of d_{21} is negative, surprisingly gain without inversion with steep anomalous dispersion could be attained. © *2009 American Institute of Physics*. [DOI: 10.1063/1.3176018]

I. INTRODUCTION

Electromagnetically induced transparency[1–8] (EIT) is an important quantum interference effect which renders a medium transparent over a narrow spectral region within an absorption line. Meanwhile, there exists steep dispersion within the transparency window. Since EIT was proposed by Harris *et al.*[1] in 1990, great efforts were made in this area and its wide applications attracted considerable attention, such as laser without inversion,[9,10] enhanced optical nonlinearity,[11,12] information storage,[13,14] etc. Up until now, there have been a large number of theoretical contributions and experimental demonstrations of EIT in atomic and molecular gases,[15,16] ion-doped crystals,[17,18] semiconductors,[19,20] and superconducting quantum devices.[21,22]

To the best of our knowledge, in all the previous works little attention has been paid to EIT in polar molecules. Many recent studies[23–27] shown that μ_{jj}, the permanent dipole moments (PDMs), can affect the molecule-laser coupling and allow transitions to occur in such media which would otherwise be forbidden. Thus not only significant differences can occur between systems with and without μ_{jj} but also new mechanisms for some phenomena can be introduced, for instance, two-photon absorption,[23] two-photon phase conjugation,[28] two-photon optical bistability,[29] and so on. Recently, Brown[30] examined stimulated Raman adiabatic passage (STIRAP) in a Λ model molecular system with PDMs μ_{jj} and a previously developed generalized rotating wave approximation[31] (RWA) was used to qualitatively interpret the calculation results. He showed that the presence of μ_{jj} can allow alternative multiphoton mechanisms for STIRAP to occur, and it was highlighted that (2+2)-STIRAP as a potential new mechanism was able to overcome the inherent detrimental effect of μ_{jj}.

In the present paper, we consider EIT in a three-level Λ system with PDMs. By using the developed RWA to describe the system theoretically, absorption and dispersion response of the medium are investigated for both the (1+1)- and (2+2)-transition processes. It will be shown that the influence of μ_{jj} on EIT behavior is significant in the case of (2+2)-transition processes where the probe and coupling processes both involve the absorption of two photons, comparing with that in the case of (1+1)-transition processes where the probe and coupling processes both involve the absorption of only one photon.

II. MODEL AND CALCULATIONS

We investigate the active medium that behaves like a three-level Λ system formed by N polar molecules, as shown in Fig. 1. A strong coupling field $\varepsilon_s(t)=\varepsilon_s \cos \omega_s t$ drives the transition $|2\rangle \leftrightarrow |3\rangle$ while a weak probe field $\varepsilon_p(t)=\varepsilon_p \cos \omega_p t$ is applied to the transition $|2\rangle \leftrightarrow |1\rangle$. The equation of motion for the state amplitude of the system at time t is expressed in the dipole approximation as

$$i\frac{\partial}{\partial t}a(t)=[\mathbf{E}-\boldsymbol{\mu}\cdot\varepsilon(t)]a(t), \tag{1}$$

where the field strength

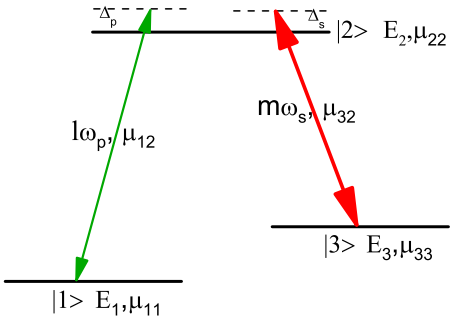

FIG. 1. Schematic of a three-level Λ system interacting with probe field of frequency ω_p and coupling field of frequency ω_s.

[a]Electronic mail: niuyp@mail.siom.ac.cn.
[b]Electronic mail: sqgong@siom.ac.cn.

$$\varepsilon(t) = \hat{e}_p \varepsilon_p \cos \omega_p t + \hat{e}_s \varepsilon_s \cos \omega_s t. \tag{2}$$

Here the energy $(\mathbf{E})_{jk}=E_j\delta_{jk}$, $\boldsymbol{\mu}$ is the projection of the electric dipole moment operator of the molecule along the field direction, and $(\boldsymbol{\mu})_{jk}=\mu_{jk}=\langle j|\mu|k\rangle$ are the permanent $(j=k)$ and transition $(j\neq k)$ dipole moments. ε_p, ω_p and ε_s, ω_s are the strengths, frequencies of the probe, and coupling fields, respectively.

As what has been done in literatures[31–34] previously, Eq. (1) is transformed to an interaction representation defined by

$$\mathbf{a}(t) = \mathbf{T}\mathbf{b}(t), \tag{3}$$

where $\mathbf{T}$ is a diagonal transformation matrix given by

$$T_{jk} = \delta_{jk} \exp[-iE_j t]\exp[i\gamma_{jk}], \tag{4}$$

and

$$\gamma_{jk} = \mu_{jk}\int_0^t \varepsilon(t')dt'. \tag{5}$$

Substitution of Eq. (3) into Eq. (2) yields

$$i\frac{\partial}{\partial t}\mathbf{b}(t) = \mathbf{H}^b(t)\mathbf{b}(t), \tag{6}$$

where $\mathbf{H}^b(t)$ is the Hamiltonian in the new representation,

$$H^b_{jk}(t) = -\mu_{jk}\varepsilon(t)\exp[-i(E_k-E_j)t]\exp[i(\gamma_{kk}-\gamma_{jj})]. \tag{7}$$

Plugging Eq. (5) into Eq. (7), expending the cosine functions in terms of exponentials, and using $\exp(iz\sin x)=\sum_{n=-\infty}^{\infty}J_n(z)\exp(inx)$, where $J_n(z)$ is the first kind Bessel function of integer order n, then gives

$$H^b_{jk}(t) = -\sum_{l=-\infty}^{\infty}\sum_{m=-\infty}^{\infty}\left(\frac{l\mu_{jk}\cdot\hat{e}_p\varepsilon_p}{z^p_{kj}}+\frac{m\mu_{jk}\cdot\hat{e}_s\varepsilon_s}{z^s_{kj}}\right) \times J_l(z^p_{kj})J_m(z^s_{kj})\exp[-i(E_{kj}-l\omega_p-m\omega_s)t], \tag{8}$$

$$z^\alpha_{kj} = \frac{d_{kj}\cdot\hat{e}_\alpha\varepsilon_\alpha}{\omega_\alpha}, \quad d_{kj}=\mu_{kk}-\mu_{jj}, \tag{9}$$

where $E_{kj}=E_k-E_j$, and α represents the note of p or s.

This is the point at which the RWA can be made. The far-off-resonant terms in the exponentials are neglected. It is assumed that the probe transition involves the absorption of l probe photons, and zero coupling photons, while the coupling transition involves the absorption of m coupling photons and zero probe photons.[30] After making the RWA, the Hamiltonian has the matrix form

$$\mathbf{H}^b(t) = -\begin{pmatrix} 0 & C_p^{(0,l)}e^{i\Delta_p t} & 0 \\ C_p^{(0,l)}e^{-i\Delta_p t} & 0 & C_s^{(m,0)}e^{-i\Delta_s t} \\ 0 & C_s^{(m,0)}e^{i\Delta_s t} & 0 \end{pmatrix}, \tag{10}$$

where

$$C_p^{(0,l)} = \frac{l\mu_{12}\varepsilon_p}{z^p_{21}}J_0(z^s_{21})J_l(z^p_{21}), \tag{11}$$

$$C_s^{(m,0)} = \frac{m\mu_{32}\varepsilon_s}{z^s_{23}}J_m(z^s_{23})J_0(z^p_{23}), \tag{12}$$

the laser-molecule couplings $C_p^{(0,l)}$ and $C_s^{(m,0)}$ are termed as the Rabi frequencies for the probe and coupling fields,[30] respectively, comparing with the situations without PDMs (i.e., $\mu_{jj}=0$). $\Delta_p=l\omega_p-E_{21}$ and $\Delta_s=m\omega_s-E_{23}$ are the probe and coupling field frequency detunings, respectively. In this work, we consider that the PDMs μ_{jj}, the transition dipole moments $\mu_{jk}(j\neq k)$, and the field polarization $\hat{e}_\alpha$ are parallel with one another.

From these expressions of Eqs. (10)–(12), it is evident that the existence of the PDMs modified the laser-molecule interaction through the Rabi frequency terms, which cause the multiphoton processes to occur, especially for the case of two-photon transitions in a two-level scheme. Moreover, although the probe (coupling) transition involves the absorption of zero coupling (probe) photons, the coupling (probe) field can affect the probe (coupling) Rabi frequency through the term $J_0(z^\alpha_{kj})$. If the argument of the Bessel function is small, e.g., d_{kj} is small, the effect of the $J_0(z^\alpha_{kj})$ can be neglected since $\lim_{z^\alpha_{kj}\to 0}J_0(z^\alpha_{kj})=1$. Then the Rabi frequencies for the probe and coupling fields are independent and can be written as

$$C_p^{(0,l)} = \frac{l\mu_{12}\varepsilon_p}{z^p_{21}}J_l(z^p_{21}), \tag{13}$$

$$C_s^{(m,0)} = \frac{m\mu_{32}\varepsilon_s}{z^s_{23}}J_m(z^s_{23}). \tag{14}$$

These two equations will be referred to as the effective Rabi frequencies.

We can derive the equations of motion for the density matrix elements from $\dot{\rho}=-i[H^b(t),\rho]-\frac{1}{2}\{\Gamma,\rho\}$ with the Hamiltonian given by Eq. (10). Making the substitutions $\rho_{21}=\sigma_{21}e^{-i\Delta_p t}$, $\rho_{32}=\sigma_{32}e^{i\Delta_s t}$, $\rho_{31}=\sigma_{31}e^{-i(\Delta_p-\Delta_s)t}$, and $\rho_{jj}=\sigma_{jj}, (j=1,2,3)$, we can obtain

$$\dot{\sigma}_{11} = \gamma_1\sigma_{22} + iC_p^{(0,l)}(\sigma_{21}-\sigma_{12}), \tag{15a}$$

$$\dot{\sigma}_{33} = \gamma_2\sigma_{22} + iC_s^{(m,0)}(\sigma_{23}-\sigma_{32}), \tag{15b}$$

$$\dot{\sigma}_{21} = (-\gamma_{21}+i\Delta_p)\sigma_{21} - iC_p^{(0,l)}(\sigma_{22}-\sigma_{11}) + iC_s^{(m,0)}\sigma_{31}, \tag{15c}$$

$$\dot{\sigma}_{31} = (-\gamma_{31}+i\Delta_p-i\Delta_s)\sigma_{31} - iC_p^{(0,l)}\sigma_{32} + iC_s^{(m,0)}\sigma_{21}, \tag{15d}$$

$$\dot{\sigma}_{32} = -(\gamma_{32}+i\Delta_s)\sigma_{32} - iC_p^{(0,l)}\sigma_{31} - iC_s^{(m,0)}(\sigma_{33}-\sigma_{22}). \tag{15e}$$

The above equations are constrained by $\sigma_{jk}=\sigma^*_{kj}$ and $\sigma_{11}+\sigma_{22}+\sigma_{33}=1$. Here γ_1 and γ_2 are the spontaneous emission rates from level $|2\rangle$ to levels $|1\rangle$ and $|3\rangle$, respectively. $\gamma_{jk}(j\neq k)$ is the coherence decay rate of the corresponding nondiagonal element. In order to use the weak probe approximation which is widely used in the conventional EIT, we truncate the infinite series of Bessel function with the

argument of probe field strength ε_p as follows:

$$J_l(z_{21}^p)=\sum_{k=0}^{\infty}\frac{(-1)^k}{k!\,(l+k)!}\left(\frac{z_{21}^p}{2}\right)^{2k+l}\approx\frac{1}{l!}\left(\frac{z_{21}^p}{2}\right)^{l}. \tag{16}$$

We assume that in the absence of the external fields the system is in equilibrium, that is, $\sigma_{11}^{(0)}=1$, $\sigma_{22}^{(0)}=\sigma_{33}^{(0)}=\sigma_{23}^{(0)}=0$. Substituting these values of the matrix elements and Eq. (16) into Eqs. (15a)–(15e), we get the following coupled set of equations:

$$\dot{\sigma}_{21}=(-\gamma_{21}+i\Delta_p)\sigma_{21}+i\frac{m\mu_{32}\varepsilon_s}{z_{23}^s}J_m(z_{23}^s)\sigma_{31}+i\frac{\mu_{12}\omega_p}{(l-1)!\,d_{21}}\left(\frac{z_{21}^p}{2}\right)^{l}, \tag{17}$$

$$\dot{\sigma}_{31}=(-\gamma_{31}+i\Delta_p-i\Delta_s)\sigma_{31}+i\frac{m\mu_{32}\varepsilon_s}{z_{23}^s}J_m(z_{23}^s)\sigma_{21}. \tag{18}$$

By solving this set of equations in steady state, we obtain

$$\sigma_{21}=\frac{\Omega_{p\mathrm{eff}}}{2}\left(\frac{\mu_{12}d_{21}(E_3-\frac{1}{2}E_2)}{\mu_{13}\mu_{32}\omega_p}\right)^{l-1}\times\frac{(\Delta_p-\Delta_s+i\gamma_{31})}{(\gamma_{21}-i\Delta_p)(\gamma_{31}-i\Delta_p+i\Delta_s)+\left(\frac{m\mu_{32}\varepsilon_s}{z_{23}^s}J_m(z_{23}^s)\right)^2}. \tag{19}$$

In this paper, only two processes are considered: one photon plus one photon transitions ($m=1$, $l=1$) and two photon plus two-photon transitions ($m=2$, $l=2$). $\Omega_{p\mathrm{eff}}=\mu_{12}\varepsilon_p$ for (1+1)-transitions and $\Omega_{p\mathrm{eff}}=[\mu_{13}\mu_{32}/(2E_3-E_2)]|\varepsilon_p|^2$ (Ref. 35) for (2+2)-transitions since the influences of all but the three states we considered here are neglected.

The polarization components with frequency ω_p can be obtained in terms of the density matrix elements σ_{21} by $P(\omega_p)=2N\mu_{12}\sigma_{21}$,[36] and then the complex susceptibility

$$\chi\propto\frac{P(\omega_p)}{\Omega_{p\mathrm{eff}}}=K\frac{\left(\frac{d_{21}}{\omega_p}\right)^{l-1}(\Delta_p-\Delta_s+i\gamma_{31})}{(\gamma_{21}-i\Delta_p)(\gamma_{31}-i\Delta_p+i\Delta_s)+\left(\frac{m\Omega_s}{z_{23}^s}J_m(z_{23}^s)\right)^2}, \tag{20}$$

where $\Omega_s=\mu_{32}\varepsilon_s$; the constant K will be given in Sec. III. As is well known, the imaginary part $\mathrm{Im}[\chi]$ and real part $\mathrm{Re}[\chi]$ of the susceptibility determine the absorption and dispersion of the system, respectively. The group velocity index is defined by

$$n_g(\omega_p)=\frac{c}{v_g}=n(\omega_p)+\omega_p\frac{dn}{d\omega_p}, \tag{21}$$

where $n(\omega_p)$ is the refractive index and $n(\omega_p)=\sqrt{1+\mathrm{Re}[\chi]}$. When $n_g-1>0$, the group velocity is smaller than the velocity of light in vacuum, which means slow light[37,38] can be attained. Contrarily, when $n_g-1<0$, the group velocity is larger than the velocity of light in vacuum, then fast light[39,40] can be obtained. We will plot the absorption $\mathrm{Im}[\chi]$ and dispersion $\mathrm{Re}[\chi]$ profiles of the medium by Eq. (20) along with the group index profiles for n_g-1 by Eq. (21) as a function of the frequency detuning of the probe field in Sec. III.

TABLE I. Energy and PDMs used in our calculations.

j	1	2	3
E_j (a.u.)	0.0	0.047(0.063)	0.023
μ_{jj} (a.u.)	1.17	1.18(1.08)	−1.17

III. RESULTS AND DISCUSSION

The molecular parameters used in our simulations are based on HCN→HNC isomerization which has often been used in theoretical studies of molecular dynamics.[41,42] Table I lists the values of the energy E_j of the three states in our model and the corresponding PDMs μ_{jj} in atomic units, which were included in earlier studies (Refs. 30 and 43). Two different values of the transition dipole moments are regarded here: 0.01 a.u. for (1+1)-transitions and 0.1 a.u. for (2+2)-transitions.[30] Although the exact data are not available for longitudinal and transversal relaxation rates, the transversal relaxation rate is fixed at 10^{12} s^{-1}, which is of the order of the reorientation rate of molecules in solution, and the longitudinal rate is considered to lie in the 10^9–10^{12} s^{-1} range.[28] These values are typical in molecular systems such as organic dyes.[44] For simplicity, the parameters of energies, frequencies, and detunings are scaled by the decay rate γ_{21} in the following numerical calculations.

In Sec. II, we have already noticed that because of the existence of diagonal dipole matrix elements μ_{jj} the Rabi frequencies are no longer proportional to the field amplitudes and it can be seen clearly from the expression of Eq. (20) that the influence of μ_{jj} on the susceptibility chiefly arise from a factor of d_{21}, the difference in PDMs of the probe states, and terms involving the Bessel functions that are oscillatory. While in the case of (1+1)-transition processes, it is obvious that the effect of d_{21} disappears although the PDMs can be very large. The complex susceptibility is

$$\chi=\frac{K_1(\Delta_p-\Delta_s+i\gamma_{31})}{(\gamma_{21}-i\Delta_p)(\gamma_{31}-i\Delta_p+i\Delta_s)+\left(\frac{\Omega_s}{z_{23}^s}J_1(z_{23}^s)\right)^2}, \tag{22}$$

where $K_1=N\mu_{12}^2/\epsilon_0$ and it is set to be unity for simplicity in our numerical simulations. N is the molecular density and ϵ_0 is the free space permittivity. Essentially, there are not too much differences between EIT of this case and the conventional ones, except for the Rabi frequency of the coupling field modified by the ratio of $J_1(z_{23}^s)/z_{23}^s$ which is oscillatory in nature, as shown in Fig. 2(a). Obviously, Bessel functions restrict the effective Rabi frequency of the coupling field strength. We choose arbitrarily three different values of the coupling field strength Ω_s marked with dots A, B, and C in Fig. 2(a) and plot the corresponding representative profiles of the imaginary part $\mathrm{Im}[\chi]$ (red solid curves) and the real part

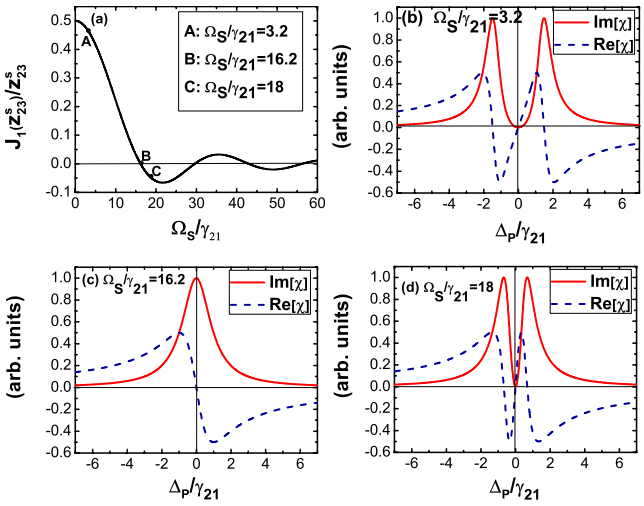

FIG. 2. Profiles for (1+1)-transition processes. (a) The oscillatory feature of the terms including Bessel functions vs the coupling field strength. [(b), (c), and (d)] Variations of Im[χ] (red solid) and Re[χ] (blue dashed) vs the probe detuning Δ_p at different coupling strengths corresponding to dots of A, B, and C in (a), respectively.

Re[χ] (blue dashed curves) of the susceptibility as a function of the probe field detuning in Figs. 2(b)–2(d), respectively. The main parameters used here are $\mu_{22}=1.18$ a.u., $\mu_{32}=0.01$ a.u., $\omega_s=E_{23}=0.024$ a.u.$=992\gamma_{21}$, $\Delta_s=0$, and $\gamma_{31}=0$.

From the profile of the imaginary part of the susceptibility Im[χ] in Fig. 2(b), it can be seen that the absorption vanishes at the probe resonance, i.e., perfect EIT has been attained. Simultaneously, a steep dispersion appears in line center as shown by the profile of Re[χ] so that the group velocity (dependent upon the slope of Re[χ]) can become anomalously low where absorption has vanished. It can been seen from Fig. 2(a) that the effective Rabi frequency can be zero at the point of B due to the Bessel function with the appropriate coupling field strength Ω_s, and in this case there is a strong absorption peak at resonance and no transparency window of EIT any more, as shown in Fig. 2(c), although the strength of the coupling field is large. Therefore, in order to get the perfect EIT, the adiabatic condition[4,30] comes to be $|(\Omega_s/z_{23}^s)J_1(z_{23}^s)|^2 \gg \gamma_{21}\gamma_{31}$ to avoid the zeros and small values of Bessel functions resulting from the detrimental effect of μ_{jj}. When this condition is satisfied EIT could be observed, as shown in Figs. 2(b) and 2(d). We also notice that the linewidth of EIT (the full width of EIT resonance at half maximum)[45] is now proportional to $(\Omega_s/z_{23}^s)J_1(z_{23}^s)$, the effective Rabi frequency of the coupling field.

We now consider the case of (2+2)-transition processes, where the coupling and probe transitions both involve the absorption of two photons. The frequencies of the coupling and probe fields are set to be $\omega_s=E_{23}/2$ and $\omega_p=(E_{21}-\Delta_p)/2$. The complex susceptibility in this case is

$$\chi=\frac{K_2\dfrac{d_{21}}{\omega_p}(\Delta_p-\Delta_s+i\gamma_{31})}{(\gamma_{21}-i\Delta_p)(\gamma_{31}-i\Delta_p+i\Delta_s)+\left(\dfrac{2\Omega_s}{z_{23}^s}J_2(z_{23}^s)\right)^2}, \quad (23)$$

where the constant $K_2=(N\mu_{12}^3/\epsilon_0\mu_{13}\mu_{32})[E_3-(1/2)E_2]$, and we set $K_2=1$ for simplicity in the following numerical calculations. Apparently, the susceptibility of the system is in proportion to d_{21}. When the sign of d_{21} is reversed, the properties of the susceptibility will change. So we consider two conditions of $d_{21}>0$ and $d_{21}<0$ in the following. The main parameters used here are $E_2=0.047$ a.u., $E_{21}=1943\gamma_{21}$, $\omega_s=496\gamma_{21}$, and $\mu_{22}=1.18$ a.u. for $d_{21}>0$ and $E_2=0.063$ a.u., $E_{21}=2604\gamma_{21}$, $\omega_s=827\gamma_{21}$, and $\mu_{22}=1.08$ a.u. for $d_{21}<0$. $\Delta_s=0$, $\gamma_{31}=0$, and $\mu_{32}=0.1$ a.u. Similar to that of the (1+1)-transition process, the EIT condition comes to be $|(2\Omega_s/z_{23}^s)J_2(z_{23}^s)|^2 \gg \gamma_{21}\gamma_{31}$, and the linewidth of EIT is manipulated by the Bessel oscillatory term $(2\Omega_s/z_{23}^s)J_2(z_{23}^s)$. Here, we focus our attention on the influence of d_{21} on the susceptibility and modulate the coupling field to satisfy the adiabatic condition. The imaginary part Im[χ] (red solid) and the real part Re[χ] (blue dashed) of the susceptibility together with the group index n_g-1 (black dashed dotted) versus the probe detuning at different Ω_s for the conditions $d_{21}>0$ and $d_{21}<0$ are presented in Figs. 3 and 4, respectively.

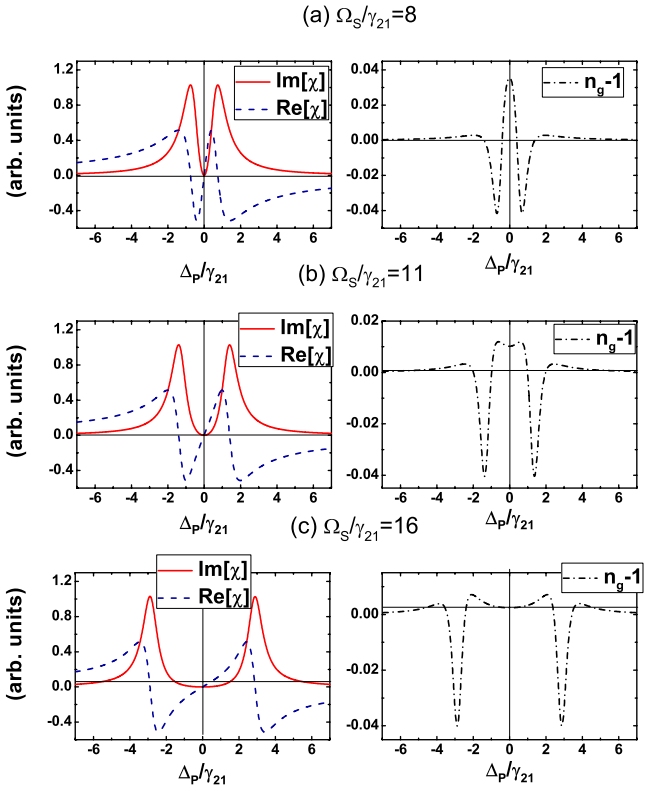

FIG. 3. Variations of Im[χ] (red solid), Re[χ] (blue dashed), and group index n_g-1 (black dashed dotted) vs the probe detuning Δ_p for the (2+2)-transition in the three-level Λ system with $d_{21}>0$ at different coupling field strengths Ω_s. The rows of (a), (b), and (c) correspond to $\Omega_s=8\gamma_{21}$, $\Omega_s=11\gamma_{21}$, and $\Omega_s=16\gamma_{21}$, respectively.

In the case of $d_{21}>0$, perfect EITs (nearly zero resonant absorption of the probe field) with steep normal dispersion are present in the left column plots of Fig. 3 at different Ω_s, where we have already chosen these Ω_s to satisfy the EIT conditions. In addition, as shown in the right column of Fig. 3 positive group index profile for n_g-1 (i.e., $v_g<c$) in the EIT window resulted by the steep normal dispersion is achieved, which is most important in the slow light.[37,38] Thus we can see that in the presence of PDMs, EIT can be avail-

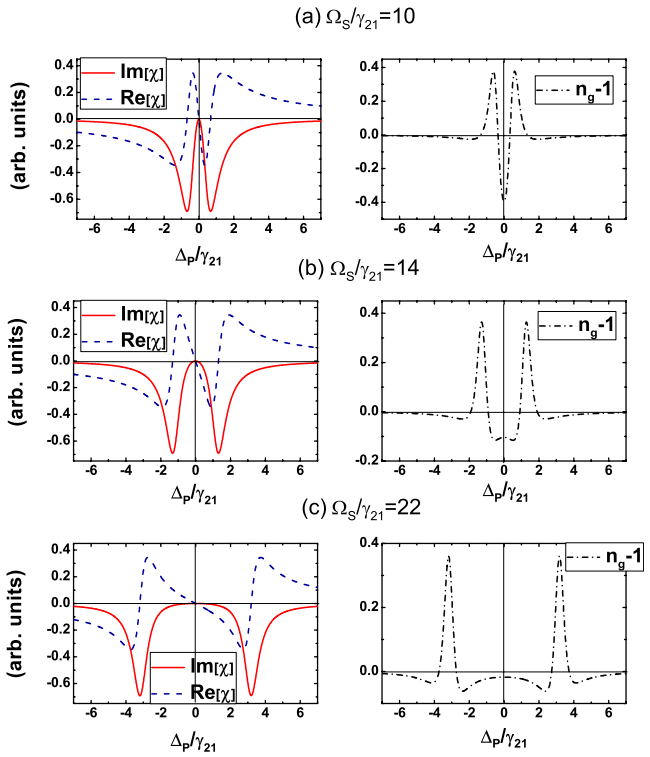

FIG. 4. Variations of Im[χ] (red solid), Re[χ] (blue dashed), and group index n_g-1 (black dashed dotted) vs the probe detuning Δ_p for the (2+2)-transition in the three-level Λ system with $d_{21}<0$ at different coupling field strengths Ω_s. The rows of (a), (b), and (c) correspond to $\Omega_s=10\gamma_{21}$, $\Omega_s=14\gamma_{21}$, and $\Omega_s=22\gamma_{21}$, respectively.

able not only by using the one photon transition but also by utilization of alternative multiphoton transition, which possess intrinsic difference from the conventional EIT in the atoms or nonpolar molecules.

In the case of $d_{21}<0$, as shown in Fig. 4, the opposite window, i.e., gain profiles with EIT at the probe resonant transition ($\Delta_p=0$) and anomalous dispersion between the two gain peaks are surprisingly gained. Furthermore, we can derive the population of the three states in steady state from Eqs. (15a)–(15e) and get $\sigma_{11}=1$ and $\sigma_{22}=\sigma_{33}=0$. That is to say, there are no population inversions between the transition states and gain without inversion (GWI) is obtained under this condition. From the right column of Fig. 4, we can see that negative group index profile for n_g-1 (i.e., $v_g>c$) caused by the anomalous dispersion at the center region which means that fast light[39,40] are achieved in this system. Of course, it can also be seen that when the width of the EIT (or GWI) window is too large, the slope of Re[χ] is too low and it is not good for slow (or fast) light.

For further understanding of the physical mechanisms leading to EIT and GWI in the (2+2)-transition processes of this system, we reconsider the expression of σ_{21} in steady state from Eqs. (15c) and (15d),

$$\sigma_{21}=\frac{iC_p^{(0,2)}\sigma_{11}+iC_s^{(2,0)}\sigma_{31}}{\gamma_{21}-i\Delta_p}, \tag{24a}$$

$$\sigma_{31}=\frac{iC_s^{(2,0)}\sigma_{21}}{\gamma_{31}-i\Delta_p+i\Delta_s}. \tag{24b}$$

The imaginary part of susceptibility can be rewritten as

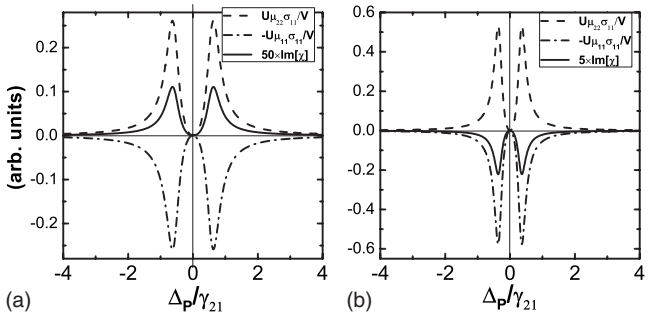

FIG. 5. Variations of the Im[χ] (solid) vs Δ_p and the contributions of $\mu_{22}\sigma_{11}$ (dashed) and $-\mu_{11}\sigma_{11}$ (dashed dotted) to Im[χ] for the absorption profile when $d_{21}>0$ in (a) and for the GWI profile when $d_{21}<0$ in (b). $\Omega_s=8\gamma_{21}$. The other parameters are the same as that in Figs. 3 and 4 respectively.

$$\mathrm{Im}[\chi]=\frac{K_2U}{V}\left(\frac{\mu_{22}}{\omega_p}\sigma_{11}-\frac{\mu_{11}}{\omega_p}\sigma_{11}\right), \tag{25}$$

where

$$U=\gamma_{21}\gamma_{31}^2+\gamma_{21}(\Delta_p-\Delta_s)^2+\gamma_{31}(C_s^{(2,0)})^2, \tag{26}$$

$$V=[\gamma_{21}\gamma_{31}-\Delta_p(\Delta_p-\Delta_s)+(C_s^{(2,0)})^2]^2+[\gamma_{31}\Delta_p+\gamma_{21}(\Delta_p-\Delta_s)]^2. \tag{27}$$

Notice that $\sigma_{22}=0$ for steady state have already been used here. Apparently, it can be seen from this equation that PDMs impact the absorption and gain of the system greatly. Im[χ] consists two terms: The first term involving the PDMs of the excited state μ_{22} in the parentheses decides the absorption while the second term involving the PDMs of the ground state μ_{11} determines the gain, as shown in Figs. 5(a) and 5(b). When $d_{21}=\mu_{22}-\mu_{11}>0$, the contributions of the absorption term are greater than that of the gain term, the system exhibits absorption profile and EIT can be attained, as shown in Fig. 5(a). Conversely, when $d_{21}=\mu_{22}-\mu_{11}<0$, the contributions of the absorption term are less than that of the gain term, the system exhibits gain profile and GWI can be obtained, as shown in Fig. 5(b). When $\mu_{jj}=0$ (or $d_{21}=0$), it will turn out to be the conventional three-level model without μ_{jj}, the atomic or nonpolar molecular system, where the two-photon transitions would be forbidden then all the phenomena in Figs. 3 and 4 will not exist, which reveal the critical role of PDMs in multiphoton EIT scenarios.

Therefore, d_{21} plays an important role in the absorption and dispersion profiles of the medium in the (2+2)-transition processes. When d_{21} changes from positive to negative, the characteristic of the window varies from EIT to GWI. Meanwhile, the properties of the dispersion in the line center is also modified from normal to anomalous, as shown in Figs. 3 and 4, thus the group index profiles change from positive to negative on resonant. These indicate that we can get slow or fast light in this system with nearly zero absorption for the probe field by exciting the molecule to different highly excited vibrational state $|2\rangle$ with specific PDMs μ_{22}. Another thing we want to emphasize is that the PDMs could lead to detrimental effect to EIT because of the induced oscillatory Bessel functions just as we have already pointed out previously, which limit the effective Rabi frequency of the cou-

pling field strength and therefore limit the role of the coupling field strength playing in the EIT processes. The tunable range of the width of EIT (or GWI) windows for getting preferable steep dispersion for slow (or fast) light is narrowing after the first oscillatory period of Bessel function when Ω_s is increasing. So it is meaningless for Ω_s being too large. Fortunately, we could attenuate this influence by controlling the coupling field strength in proper range.

IV. CONCLUSION

In summary, we have investigated EIT in a three-level Λ molecular system with nonzero PDMs μ_{jj}. The developed RWA is used to deal with the absorption and dispersion properties of this system applied with a weak probe field and an intense coupling field. Two processes of (1+1) and (2+2) transition have been considered here. It has been shown that there are not too much differences for EIT between systems with and without PDMs in the (1+1)-transition processes, and the existence of the μ_{jj} only leads to not good effect for EIT by restricting the effective coupling field strength. Nevertheless, in the (2+2)-transition case, not only perfect EIT is achieved but also GWI is gained near the probe resonant point under adiabatic conditions, which is mainly determined by d_{21}, the difference in the PDMs of the probe states. When the sign of d_{21} is reversed from positive to negative, the feature of the absorption curves changes from EIT to GWI. Meanwhile, the dispersion profile at the line center changes from steep normal to anomalous, which means that a transfer between slow and fast light for the system can be gained by utilizing special highly excited vibrational state $|2\rangle$ in the Λ system owning particular PDMs μ_{22}. We hope that our results will not only motivate future studies of EIT but also expand the applications of the polar molecules.

ACKNOWLEDGMENTS

We sincerely acknowledge constructive correspondence with Professor Jiangbin Gong of the Department of Physics of National University of Singapore. This work was supported by the National Natural Science Foundation of China with Grant Nos. 10874194, 60708008, and 60878009, the National Basic Research Program of China (973 Program) with Grant No. 2006CB921104, the Key Basic Research foundation of Shanghai with Grant No. 08JC1409702, and the Project of Academic Leaders in Shanghai with Grant No. 07XD14030.

[1] S. E. Harris, J. E. Field, and A. Imamoğlu, Phys. Rev. Lett. **64**, 1107 (1990).
[2] S. E. Harris, Phys. Today **50**(7), 36 (1997).
[3] J. P. Marangos, J. Mod. Opt. **45**, 471 (1998).
[4] M. Fleischhauer, A. Imamoğlu, and J. P. Marangos, Rev. Mod. Phys. **77**, 633 (2005).
[5] K. J. Boller, A. Imamoğlu, and S. E. Harris, Phys. Rev. Lett. **66**, 2593 (1991).
[6] K. Hakuta, L. Marmet, and B. P. Stoicheff, Phys. Rev. Lett. **66**, 596 (1991).
[7] K. Hakuta, L. Marmet, and B. P. Stoicheff, Phys. Rev. A **45**, 5152 (1992).
[8] M. Xiao, Y. Li, S. Jin, and J. Geabanacloche, Phys. Rev. Lett. **74**, 666 (1995).
[9] H. M. Doss, L. M. Narducci, M. O. Scully, and J. Y. Gao, Opt. Commun. **95**, 57 (1993).
[10] A. S. Zibrov, M. D. Lukin, D. E. Nikonov, L. Hollberg, M. O. Scully, V. L. Vechansky, and H. G. Robinson, Phys. Rev. Lett. **75**, 1499 (1995).
[11] C. Dorman, I. Kucukkara, and J. P. Marangos, Phys. Rev. A **61**, 013802 (1999).
[12] H. S. Kang, G. Hernandez, and Y. F. Zhu, J. Mod. Opt. **52**, 2391 (2005).
[13] M. Fleischhauer and M. D. Lukin, Phys. Rev. Lett. **84**, 5094 (2000).
[14] A. Raczynski and J. Zaremba, Opt. Commun. **209**, 149 (2002).
[15] J. Qi, F. C. Spano, T. Kirova, A. Lazoudis, J. Magnes, L. Li, L. M. Narducci, R. W. Field, and A. M. Lyyra, Phys. Rev. Lett. **88**, 173003 (2002).
[16] A. Lazoudis, E. H. Ahmed, L. Li, T. Kirova, P. Qi, A. Hansson, J. Magnes, and A. M. Lyyra, Phys. Rev. A **78**, 043405 (2008).
[17] B. S. Ham, M. S. Shahriar, and P. R. Hemmer, Opt. Lett. **22**, 1138 (1997).
[18] B. S. Ham, P. R. Hemmer, and M. S. Shahriar, Opt. Commun. **114**, 227 (1997).
[19] F. Bassani, G. C. La Rocca, and M. Artoni, J. Lumin. **110**, 174 (2004).
[20] P. K. Nielsen, H. Thyrrestrup, J. Mørk, and B. Tromborg, Opt. Express **15**, 6396 (2007).
[21] K. V. R. M. Murali, Z. Dutton, W. D. Oliver, D. S. Crankshaw, and T. P. Orlando, Phys. Rev. Lett. **93**, 087003 (2004).
[22] Z. Dutton, K. V. R. M. Murali, W. D. Oliver, and T. P. Orlando, Phys. Rev. B **73**, 104516 (2006).
[23] D. F. Heller and Y. B. Band, Phys. Rev. A **41**, 3960 (1990).
[24] A. E. Kondo, V. M. Blokker, and W. J. Meath, J. Chem. Phys. **96**, 2544 (1992).
[25] A. Brown and W. J. Meath, Phys. Rev. A **53**, 2571 (1996).
[26] L. C. D. Romero and D. L. Andrews, J. Phys. B **32**, 2277 (1999).
[27] C. A. Marx and W. Jakubetz, J. Chem. Phys. **125**, 234103 (2006).
[28] M. A. Anton and I. Gonzalo, J. Opt. Soc. Am. B **8**, 1035 (1991).
[29] M. A. Anton and I. Gonzalo, IEEE J. Quantum Electron. **31**, 1088 (1995).
[30] A. Brown, Chem. Phys. **342**, 16 (2007).
[31] S. Nakai and W. J. Meath, J. Chem. Phys. **96**, 4991 (1992).
[32] M. A. Kmetic, R. A. Thuraisingham, and W. J. Meath, Phys. Rev. A **33**, 1688 (1986).
[33] W. L. Meerts, I. Ozier, and J. T. Hougen, J. Chem. Phys. **90**, 4681 (1989).
[34] A. Brown, W. J. Meath, and P. Tran, Phys. Rev. A **63**, 013403 (2000).
[35] J. C. Petch, C. H. Keitel, P. L. Knight, and J. P. Marangos, Phys. Rev. A **53**, 543 (1996).
[36] M. O. Scully and M. S. Zubairy, *Quantum Optics* (Cambridge University Press, London, 1997).
[37] M. F. Yanik, W. Suh, Z. Wang, and S. H. Fan, Phys. Rev. Lett. **93**, 233903 (2004).
[38] A. Lezama, A. M. Akulshin, A. I. Sidorov, and P. Hannaford, Phys. Rev. A **73**, 033806 (2006).
[39] L. J. Wang, A. Kuzmich, and A. Dogariu, Nature (London) **406**, 277 (2000).
[40] M. D. Stenner, D. J. Gauthier, and M. A. Neifeld, Nature (London) **425**, 695 (2003).
[41] J. B. Gong, A. Ma, and S. A. Rice, J. Chem. Phys. **122**, 144311 (2005).
[42] J. B. Gong, A. Ma, and S. A. Rice, J. Chem. Phys. **122**, 204505 (2005).
[43] J. M. Bowman, S. Irle, K. Morokuma, and A. Wodtke, J. Chem. Phys. **114**, 7923 (2001).
[44] J. P. Lavoine, J. Chem. Phys. **127**, 094107 (2007).
[45] A. Javan, O. Kocharovskaya, H. Lee, and M. O. Scully, Phys. Rev. A **66**, 013805 (2002).